ANALYSIS OF DYNAMICAL SYSTEM BEHAVIORS OF LOOP HEAT PIPES

Triem T. Hoang
TTH Research Inc.

ABSTRACT

Loop Heat Pipes (LHPs) belong to a special class of two-phase capillary-pumped heat transport devices. Like a traditional heat pipe, LHPs do not contain mechanical moving part to wear out or break down, hence, they have become the mainstay of space thermal control systems (TCS) in the last 25 years. In the early days, during which the LHP design and intended usage was simple and straightforward, the technology contributed to the success of a string of space programs. As a consequence, LHPs were naively perceived "similar" to the heat pipes in terms of operational controllability/stability. In the first decade of this century, never-observed-before behaviors of LHP suddenly appeared – only for certain combinations of operating conditions – including self-excited oscillations of temperatures which occasionally led to the system failures. The present author suspected that the LHP dynamics were far more convoluted than those of heat pipes; involving complex processes associated with fluid flow, heat/mass transfer, phase change, buoyancy, capillary action, and perhaps more – a nonlinear dynamical system, nonetheless. In the 2011-2012 time frame, the author proposed/formulated a linear stability/instability theory for LHP operations and then spent the next 5 years to verify it against available 1-g test data from LHPs of different designs and operating regimes. The research endeavor was an unqualified success! However, a linearized stability theory of a system could only predict whether the system would become stable/unstable in a long-term operation but is not capable of predicting its behaviors once instability occurs. To reveal whether an instability would result in an unconstraint growth or oscillation (with finite amplitudes) of some parameter, Computational Fluid Dynamics (CFD) is perhaps the only method that can resolve the LHP unstable behaviors with fidelity. At the present, the lack of LHP-specific computer software compels the thermal analysts to rely on "all-purpose" commercial codes to simulate the system performance on-orbit. Being versatile, the codes have to use "brute force" to solve the governing equations in the most basic form without simplification/omission of terms due to unique properties of a particular problem. The net effect is that a reasonable LHP simulation for a typical TCS might take hours (if not days) to complete. In this paper, an analytical approach leveraging the perturbation theory multi-scale method is proposed for studying of the LHP dynamical system behaviors.

NOMENCLATURE

A_B = cross-sectional area of bayonet tube
A_{CL} = cross-sectional area of condenser line
A_{LL} = cross-sectional area of liquid line
c_P = specific heat of working fluid

$g_C^{(2\phi)}$ = condenser thermal conductance per unit volume in two-phase section

G_E = vapor-to-wall thermal conductance in evaporator

G_{L-A} = reservoir liquid-to-ambient thermal conductance (including thermal insulation)

G_{R-A} = reservoir wall-to-ambient thermal conductance (including thermal insulation)

$G_R^{(L)}$ = vapor-to-liquid thermal conductance in reservoir

$G_R^{(W)}$ = vapor-to-wall thermal conductance in reservoir

L_B = length of bayonet tube

L_{CL} = length of condenser line

L_{LL} = length of liquid line

$\dot{m}_L$ = mass flow rate in LHP liquid side

$(Mc_P)_E$ = thermal mass of evaporator including attached payload

$(Mc_P)_R^{(L)}$ = thermal mass of liquid in reservoir + portion of metal wall in contact with liquid

$(Mc_P)_R^{(W)}$ = thermal mass of vapor in reservoir + portion of reservoir wall in contact with vapor

P_E = pressure at primary wick outer surface

P_E = pressure in reservoir

$\dot{Q}_1$ = heat transported from evaporator to condensers via vapor line

$\dot{Q}_2$ = heat leak by conduction across primary wick

$\dot{Q}_C^{(2\phi)}$ = amount of heat removal by condensation at condenser

$\dot{Q}_E$ = amount of transfer from evaporator wall to LHP

$\dot{Q}_{IN}$ = heat load applied to attached payload

$\dot{Q}_R^{(L)}$ = amount of heat exchange between reservoir liquid and vapor

$\dot{Q}_R^{(W)}$ = amount of heat exchange between reservoir wall and vapor

$\dot{Q}_{SC}^{(MAX)}$ = maximum amount of return liquid subcooling available

$R_B^{(L)}$ = liquid flow resistance of bayonet tube

$R_{CL}^{(L)}$ = liquid flow resistance of liquid portion of condenser line

$R_{LL}^{(L)}$ = liquid flow resistance of liquid line

T_{AMB} = ambient temperature

$T_L^{(IN)}$ = return liquid temperature at reservoir inlet

$T_R^{(L)}$ = reservoir liquid temperature

$T_{SAT}^{(E)}$ = saturation temperature on outer surface of primary wick

$T_{SAT}^{(R)}$ = saturation temperature in reservoir

T_{SINK} = condenser sink temperature

$T_W^{(E)}$ = wall temperature of evaporator

$T_R^{(W)}$ = reservoir wall temperature

V_C = volume of condenser

$V_C^{(2\phi)}$ = volume of two-phase section of condenser

V_{RES} = vapor volume of reservoir when loop is fully flooded

V_{VL} = volume of vapor line + vapor grooves in evaporator pump + pump outlet

$\mathcal{V}_L$ = volumetric position of liquid particle relative to liquid-vapor interface

ΔT_{SC} = $T_{SAT}^{(R)} - T_L^{(IN)}$

ΔT_{VCL} = pressure difference between evaporator vapor grooves and liquid vapor interface

η = vapor-to-liquid heat exchange efficiency of bayonet tube

λ = latent heat of vaporization of LHP fluid

ρ_L = liquid density of working fluid

ρ_V = vapor density of working fluid

τ_X = time constants in Eqs. (1a)–(8a) with X = 1, 2,…, 8

τ_{LEO} = orbital period of Low-Earth-Orbit satellites

INTRODUCTION

Loop Heat Pipes (LHPs) are passive capillary-pumped heat transport devices that contain no mechanical moving parts to wear out or break down. Circulation of the working fluid in a hermetically-sealed loop and the resulting thermal/fluid dynamics are driven solely by the thermal conditions of the system environment[1,2]. A functional schematic of the LHP is shown in Figure 1. Due to its design simplicity and operational reliability/robustness, the LHP technology has gained acceptance and increasing popularity among the American spacecraft thermal engineers since its introduction to the U.S.A. in the late 1990s. Following a string of early successful space thermal control systems[3,4] (TCS), it was prematurely proclaimed – in some quarters – fully flight qualified, achieving the Technology Readiness Level (TRL) of 9. The faulty confidence emboldened the engineers to push the design envelope with operations never attempted before without sufficient analysis/testing. In the early 2000s, reports of the temperature oscillations (see Figures 2 and 3) in certain operational regimes began to appear, even when the surrounding conditions were kept constant[5,6]. In some cases, the temperature oscillations lead to the system failures[7]. Suspecting that the self-excited oscillations were perhaps a byproduct of instability common to many dynamical systems[8,9]. Scrutinizing the partial differential equations governing the heat transfer and fluid flow processes in the LHP, the author was able to derive the system operational stability/

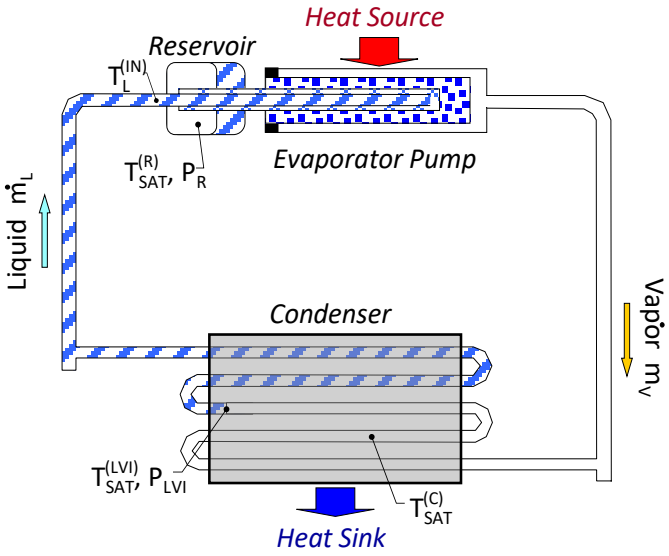

Figure 1. Schematic of Loop Heat Pipe.

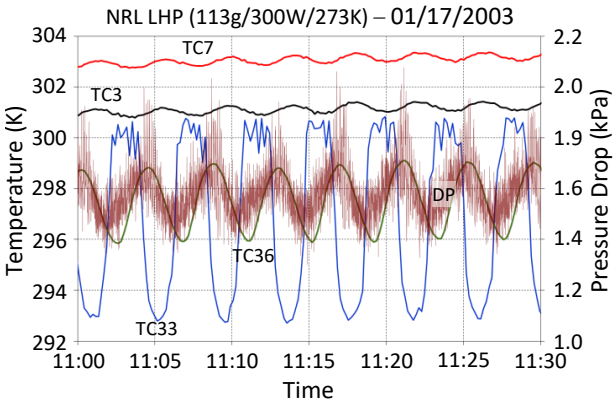

Figure 2. High Frequency Low Amplitude.

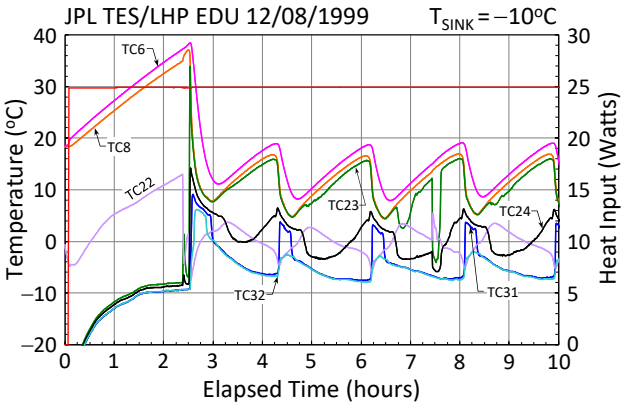

Figure 3. Low Frequency High Amplitude.

instability criteria based upon a linearization approach[10]. The said criteria were experimentally verified against LHP data from of various designs, sizes, and working fluid[11,12]. However, a linear stability theory only predicts whether stability/instability exists in an operating particular regime. So, when instability occurs, the linear theory is not capable of revealing what happens to the system performance after that. In real LHP applications, the system temperature oscillations might not be detrimental to the TCS if the oscillation characteristics are deemed acceptable within the operational limits determined by testing or analysis. Thermal testing of a flight TCS for 0-g qualification is prohibitive expensive especially when so many performance scenarios are possible during the system lifetime. So, analytical simulations are the only sensible option (of course, to be backed by limited testing for sanity check). At the present, lack of LHP-specific computer software compels the thermal analysts to rely on "all-purpose" commercial codes to simulate the system performance on-orbit. Being versatile, the codes have to use "brute force" to solve the governing equations in the most basic form (without the simplification/ omission of terms afforded by unique features of the LHP technology). The net effect is that a simple LHP simulation for a typical space TCS operation may take hours (if not days) of runtime to complete. In this paper, the author – leveraging the Perturbation Theory[13] *multi-scale method* – proposes a new paradigm in a stable and runtime efficient solution method for studying of the complex LHP dynamical system behaviors.

GOVERNING EQUATIONS

The differential equations governing the LHP thermal/fluid dynamics[14] are given below:

$$\frac{dV_C^{(2\phi)}}{dt} = \frac{1}{\rho_L}\left(-\frac{\dot{Q}_C^{(2\phi)}}{\lambda} + \dot{m}_L\right) \tag{1}$$

$$\frac{d\dot{m}_L}{dt} = \frac{P_{LVI} - P_{SAT}\left(T_{SAT}^{(R)}\right) - \left[R_B^{(L)} + R_{LL}^{(L)} + R_{CL}^{(L)}\left(1 - \frac{V_C^{(2\phi)}}{V_C}\right)\right]\dot{m}_L}{\left[\frac{L_B}{A_B} + \frac{L_{LL}}{A_{LL}} + \frac{L_{CL}}{A_{CL}}\left(1 - \frac{V_C^{(2\phi)}}{V_C}\right)\right]} \tag{2}$$

$$\frac{dT_{SAT}^{(E)}}{dt} = \frac{1}{\left(\frac{\partial \rho_V}{\partial T}\right)_{SAT}\left(V_{VL} + V_C^{(2\phi)}\right)}\left(\frac{\dot{Q}_1 - \dot{Q}_C^{(2\phi)}}{\lambda} - \rho_E^{(V)}\frac{dV_C^{(2\phi)}}{dt}\right) \tag{3}$$

$$\frac{dT_{SAT}^{(R)}}{dt} = \frac{1}{\left(\frac{\partial \rho_V}{\partial T}\right)_{SAT}\left(V_{LHP}^{(V)} - V_{VL} - V_C^{(2\phi)}\right)}\left(\frac{-\eta\dot{Q}_{SC}^{(MAX)} + \dot{Q}_2 + \dot{Q}_R^{(W)} + \dot{Q}_R^{(L)}}{\lambda} + \rho_R^{(V)}\frac{dV_C^{(2\phi)}}{dt}\right) \tag{4}$$

$$\frac{dT_W^{(E)}}{dt} = \frac{\dot{Q}_{IN} - \dot{Q}_E}{(Mc_P)_E} \tag{5}$$

$$\frac{dT_W^{(R)}}{dt} = \frac{-\dot{Q}_R^{(W)} - G_{R-\infty}(T_W^{(R)} - T_\infty)}{(Mc_P)_R^{(W)}} \tag{6}$$

$$\frac{dT_L^{(R)}}{dt} = \frac{-\dot{Q}_R^{(L)} - G_{L-\infty}\left(T_L^{(R)} - T_\infty\right) - (1-\eta)\dot{Q}_{SC}^{(MAX)}}{(Mc_P)_R^{(L)}} \tag{7}$$

$$\frac{\partial h_F}{\partial t} + \frac{\dot{m}_L}{\rho_F}\frac{\partial h_F}{\partial \square} + \frac{4h_{F-\infty}}{D\rho_F}(T_F - T_\infty) = 0 \tag{8}$$

Eq. (8) can be approximated by the following system of ordinary differential equations (ODEs) if the fluid flow is numerically represented by the lumped-parameter method.

$$M_F^{(i)}\frac{dh_F^{(i)}}{dt} + \dot{m}_L\left(h_F^{(i-1)} - h_F^{(i)}\right) + G_{F-W}^{(i)}\left(T_F^{(i)} - T_W^{(i)}\right) = 0 \qquad \text{for } i = 1 \text{ to } N_F \tag{9}$$

where,

$$\dot{Q}_E = G_E\left(T_W^{(E)} - T_{SAT}^{(E)}\right) \quad \dot{Q}_R^{(W)} = G_R^{(W)}\left(T_W^{(R)} - T_{SAT}^{(R)}\right) \quad \dot{Q}_R^{(L)} = G_R^{(L)}\left(T_L^{(R)} - T_{SAT}^{(R)}\right)$$

$$\dot{Q}_2 = UA_W\left(T_{SAT}^{(E)} - T_{SAT}^{(R)}\right)$$

$$\dot{Q}_1 = \dot{Q}_E - \dot{Q}_2 \qquad \Delta P_{VCL} = \left(R_{VL}^{(V)} + R_{CL}^{(V)}\frac{V_C^{(2\phi)}}{V_C}\right)\left(\frac{\dot{Q}_1}{\lambda}\right)^{\frac{7}{4}} \qquad P_{LVI} = P_{SAT}\left(T_{SAT}^{(E)}\right) - \Delta P_{VCL}$$

$$\dot{Q}_C^{(2\phi)} = g_C^{(2\phi)}V_C^{(2\phi)}\left(T_{SAT}^{(E)} - T_{SINK}\right) \qquad \dot{Q}_{SC}^{(MAX)} = \begin{cases} \dot{m}_L c_P\left(T_{SAT}^{(R)} - T_L^{(IN)}\right) & \text{if } \dot{m}_L > 0 \\ 0 & \text{otherwise} \end{cases}$$

The fluid mass flow rate anywhere inside the LHP is determined by Eq. (1), while the local fluid pressure variation is calculated by Eq. (4). The fluid saturation temperatures in the loop evaporator and the reservoir are regulated by the energy balance of Eqs. (3) and (4), respectively. Eqs. (5) □ (8), which belong to a larger system of thermal network surrounding the loop, govern

the heat flow in/out of the fluid control volume (i.e. across the component inner surface). The above governing equations are extremely "stiff" due to the fast-responding nature of the fluid saturation condition with respect to pressure variation. To appreciate the difficulty in solving stiff differential equations, LHP test data presented revealed a great disparity in time constants between the LHP thermal and fluid dynamic processes. The fluid and thermal time constants τ_F / τ_T are typically in the range of 0.1-0.001 seconds and 1-10 minutes, respectively. In addition, the thermal environment of a spacecraft may change periodically with time, e.g. τ_{LEO} = 1.65 hours in Low-Earth-Orbit (LEO) or τ_{GEO} = 24 hours in Geosynchronous Equatorial Orbit (GEO). Naively solving Eqs. (1)−(8) for an anticipated space simulation in the current form by any CFD method would require the integration time step to be much less than the smallest time scale. As a result, the CFD analysis is still burdensome and costly.

Recognizing that each mentioned time constant is distinctly smaller (or larger) than the rest ($\tau_F << \tau_T << \tau_{LEO}$), the method of *Multi-Scale Perturbation* is the sensible choice for obtaining the solution of Eqs. (1a) – (8a) efficiently. To bring out the time constants, the independent and dependent variables are non-dimensionalized w.r.t. a common set of parameters as follows:

$$t = \frac{M_{LHP}^{(F)}\lambda_{@293K}}{G_E\Delta T_{REF}}\bar{t} \qquad T = T_{LO} + \Delta T_{REF}\bar{T} \qquad \hbar = \hbar_{L,SAT}^{(@293K)} + \Delta\hbar_{REF}\bar{\hbar} \qquad P = \Delta P_{REF}\bar{P}$$

$$\rho = \rho_{REF}\bar{\rho} \qquad V = V_{LHP}\bar{V} \qquad \xi = V_{LHP}\bar{\xi} \qquad G = G_E\bar{G} \qquad g = \frac{G_E}{V_{LHP}}\bar{g}$$

$$\dot{\mho} = \frac{G_E\Delta T_{REF}}{\rho_{REF}\lambda_{@293K}}\bar{\dot{\mho}} \qquad \dot{Q} = G_E\Delta T_{REF}\bar{\dot{Q}} \qquad \dot{m} = \frac{G_E\Delta T_{REF}}{\lambda_{@293K}}\bar{\dot{m}} \qquad R = \frac{\Delta P_{REF}\lambda_{@293K}}{G_E\Delta T_{REF}}\bar{R}$$

$$D = D_{REF}\bar{D} \qquad \lambda = \lambda_{@293K}\bar{\lambda} \qquad c_P = \frac{\lambda_{@293K}}{\Delta T_{REF}}\bar{c}_P$$

$$\Delta T_{REF} = \frac{\dot{Q}_{MAX}}{G_E} \qquad \Delta P_{REF} = \frac{2\sigma_{@293K}}{r_P} \qquad A_{REF} = \left[\frac{(G_E\Delta T_{REF})^2 V_{LHP}}{M_{LHP}^{(F)}\lambda_{@293K}^2\Delta P_{REF}}\right]^{1/2}$$

$$G_E = \pi D_{Evap}^2 D_{Evap} 9\frac{kW}{m^2K} \qquad D_{REF} = \left(\frac{4}{\pi}A_{REF}\right)^{1/2} \qquad \rho_{REF} = \frac{M_{LHP}^{(F)}}{V_{LHP}} \qquad \Delta\hbar_{REF} = \lambda_{@293K}$$

The resulting nondimensional set of governing equations are given below:

$$\frac{d\bar{V}_C^{(2\phi)}}{d\bar{t}} = \frac{1}{\bar{\rho}_L}\left(-\bar{\dot{Q}}_C^{(2\phi)} + \bar{\dot{m}}_L\right) \tag{1a}$$

$$\tau_2\frac{d\bar{\dot{m}}_L}{d\bar{t}} = \frac{\bar{P}_{LVI} - \bar{P}_{SAT}\left(\bar{T}_{SAT}^{(R)}\right) - \left[\bar{R}_B^{(L)} + \bar{R}_{LL}^{(L)} + \bar{R}_{CL}^{(L)}\left(1 - \frac{\bar{V}_C^{(2\phi)}}{\bar{V}_C}\right)\right]\bar{\dot{m}}_L}{\left[\frac{\bar{L}_B}{\bar{A}_B} + \frac{\bar{L}_{LL}}{\bar{A}_{LL}} + \frac{\bar{L}_{CL}}{\bar{A}_{CL}}\left(1 - \frac{\bar{V}_C^{(2\phi)}}{\bar{V}_C}\right)\right]} \tag{2a}$$

$$\tau_3 \frac{d\overline{T}_{SAT}^{(E)}}{d\bar{t}} = \frac{1}{\left(\frac{\partial\bar{\rho}_V}{\partial\overline{T}}\right)_{SAT}\left(\overline{V}_{VL} + \overline{V}_C^{(2\phi)}\right)}\left(\frac{\dot{\overline{Q}}_1 - \dot{\overline{Q}}_C^{(2\phi)}}{\bar{\lambda}} - \bar{\rho}_E^{(V)}\frac{d\overline{V}_C^{(2\phi)}}{d\bar{t}}\right) \tag{3a}$$

$$\tau_4 \frac{dT_{SAT}^{(R)}}{dt} = \frac{1}{\left(\frac{\partial\bar{\rho}_V}{\partial\overline{T}}\right)_{SAT}\left(\overline{V}_{LHP}^{(V)} - \overline{V}_{VL} - \overline{V}_C^{(2\phi)}\right)}\left(\frac{-\eta\dot{\overline{Q}}_{SC}^{(MAX)} + \dot{\overline{Q}}_2 + \dot{\overline{Q}}_R^{(W)} + \dot{\overline{Q}}_R^{(L)}}{\bar{\lambda}} + \bar{\rho}_R^{(V)}\frac{d\overline{V}_C^{(2\phi)}}{d\bar{t}}\right) \tag{4a}$$

$$\tau_5 \frac{d\overline{T}_W^{(E)}}{d\bar{t}} = \dot{\overline{Q}}_{IN} - \dot{\overline{Q}}_E \tag{5a}$$

$$\tau_6 \frac{d\overline{T}_W^{(R)}}{d\bar{t}} = -\dot{\overline{Q}}_R^{(W)} - \overline{G}_{R-\infty}(\overline{T}_W^{(R)} - \overline{T}_\infty) \tag{6a}$$

$$\tau_7 \frac{d\overline{T}_L^{(R)}}{d\bar{t}} = -\dot{\overline{Q}}_R^{(L)} - \overline{G}_{L-\infty}\left(\overline{T}_L^{(R)} - \overline{T}_\infty\right) - (1-\eta)\dot{\overline{Q}}_{SC}^{(MAX)} \tag{7a}$$

$$\frac{\partial\bar{h}_F}{\partial\bar{t}} + \dot{\bar{m}}_L\frac{\partial\bar{h}_F}{\partial\bar{\xi}} + \bar{g}_{F-\infty}(\overline{T}_F - \overline{T}_\infty) = 0 \tag{8a}$$

As seen above, each of the corresponding time constants of Eqs. (1a) – (8a); designated τ_1, τ_2, …, τ_8; have a value of its own value which are listed below:

$$\tau_1 = \frac{M_{LHP}^{(F)}\lambda_{@293K}}{G_E\Delta T_{REF}} \qquad \tau_2 = \frac{2}{\frac{(\pi A_{REF})^{1/2}}{\Delta P_{REF}M_{LHP}^{(F)}}} \qquad \tau_3 = \frac{V_{LHP}\Delta T_{REF}\left(\frac{\partial\rho_V}{\partial T}\right)_{@293K}}{M_{LHP}^{(F)}} \qquad \tau_4 = \tau_3$$

$$\tau_5 = \frac{(Mc_P)_E\Delta T_{REF}}{M_{LHP}^{(F)}\lambda_{@293K}} \qquad \tau_6 = \frac{(Mc_P)_R^{(W)}}{M_{LHP}^{(F)}\lambda_{@293K}} \qquad \tau_7 = \frac{(Mc_P)_R^{(L)}}{M_{LHP}^{(F)}\lambda_{@293K}} \qquad \tau_8 = \tau_1$$

τ_2, τ_3, τ_4 are considerably smaller than τ_1 which, in turn, much less than τ_5, τ_6, τ_7 and the orbital period τ_{LEO}. For a fluid activity driven strictly by heat transferred from the ambient environment (via solid casings of the components), the system dynamics undergo gradual/smooth transition from one ambient condition to another. The reason is that the component thermal masses would damp out even sudden step changes in the operating conditions. In other words, for LHPs, the time derivatives

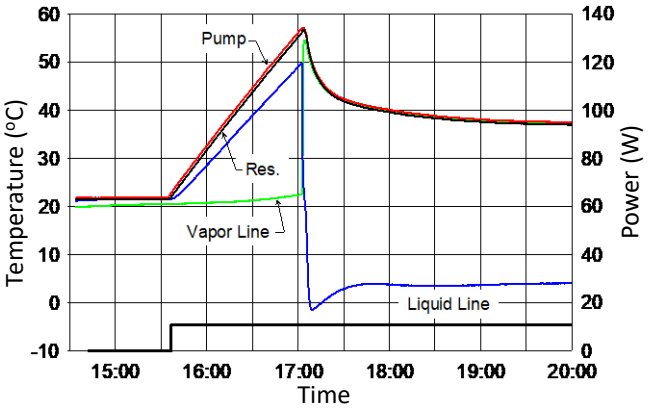

Figure 4. NRL LHP Low Power Start-up.

on the left hand sides (LHS) of Eqs. (5)−(7) likely have, for the most part, the same order of magnitude (often much less) as those of the right hand sides (RHS). Thus, there is a temptation to neglect the LHS of Eqs. (5)−(7) to reduce them to algebraic equations. It is perhaps acceptable if the time derivatives are known – *a priori or a posteriori* – to be of Order (1) or less within the computational domain. However, it is not recommended when the magnitudes of the said time derivatives are not evident beforehand. As an example, the transient dynamics of a LHP start-up are so violent that the time derivatives of Eqs. (5)−(7) spike up in magnitude for a brief period of time as recorded in an actual CPL start-up test[15] (see Figure 4).

PERTURBATION THEORY – METHOD OF MULTIPLE SCALES

The method of multi-scales[16] of perturbation theory seeks an asymptotic series solution for the integrated system of LHP and thermal surrounding. Simply put, the central idea of the method is to decompose the highly coupled thermal/ fluid system of differential equations into two separate sets, each can be integrated in time independently of the other. Appropriately enough, one for the fast-responding/fast-fading nature of the fluid dynamics and the other for the slow-pacing nature of the thermal network (including solid casings of the LHP components). Effects of a small disturbance on the thermodynamic state of the working fluid are "felt" almost immediately throughout the loop but temperatures of the thermal network remain the same (i.e. they simply do not have time to change) in the short time-scale solution or the "inner" solution. On the other hand, by the time the solution advances to the "outer" long time scale, the fluid disturbances vanish identically (i.e. the homogeneous part of the fluid solution is reduced to zero even though its particular part still persists) revealing the apparent time evolution of the thermal network temperatures in this time scale. The two (2) sets of equations are to be solved successively providing that the combined solution satisfy the initial and boundary conditions of the overall system. In addition, the inner and outer solutions have to converge (or match) in the *in-between* the time regions for uniform validity. Eqs. (1)−(8) in dimensionless form are rewritten to be valid for every element in a network of finite-difference control volumes as shown below:

$$\frac{d\overline{T}_k}{d\bar{t}} = G_j(\overline{T}_k, \overline{T}'_k, \overline{X}_i, \overline{X}'_i, \overline{X}_j, \overline{X}'_j, \bar{t}) \qquad \text{for Thermal Nodes k's in time scale } t_{REF}$$

$$\varepsilon\frac{d\overline{X}_i}{d\bar{t}} = F_i(\overline{T}_k, \overline{T}'_k, \overline{X}_i, \overline{X}'_i, \overline{X}_j, \overline{X}'_j, \bar{t}) \qquad \text{for LHP liquid nodes i's in time scale } \varepsilon t_{REF}$$

$$\varepsilon^2\frac{d\overline{X}_j}{d\bar{t}} = F_j(\overline{T}_k, \overline{T}'_k, \overline{X}_i, \overline{X}'_i, \overline{X}_j, \overline{X}'_j, \bar{t}) \qquad \text{for LHP vapor nodes j's in time scale } \varepsilon^2 t_{REF}$$

The following problem setup is for the method of multi-scale solution uniformly valid to the time scale of $\bar{t}$ = Order (ε^2) but an almost identical procedure can be extended to a system of any number of time scales. Let $\bar{t}$ be a linear combination of all time scales and the dependent variables be expressed in terms of asymptotic expansion series as shown below:

$$\bar{t} = \bar{\tau}_0 + \frac{\bar{\tau}_1}{\varepsilon} + \frac{\bar{\tau}_2}{\varepsilon^2} \qquad \Rightarrow \quad \frac{d}{d\bar{t}} = \left(\frac{\partial}{\partial\bar{\tau}_0} + \varepsilon\frac{\partial}{\partial\bar{\tau}_1} + \varepsilon^2\frac{\partial}{\partial\bar{\tau}_2}\right)$$

$$\overline{T}_k = \overline{T}_k^{(0)} + \varepsilon\overline{T}_k^{(1)} + \varepsilon^2\overline{T}_k^{(2)} \qquad \overline{T}_k^{(0)}, \overline{T}_k^{(1)}, \overline{T}_k^{(2)} \text{ are all of Order(1)}$$

$$\overline{X}_i = \overline{X}_i^{(0)} + \varepsilon\overline{X}_i^{(1)} + \varepsilon^2\overline{X}_i^{(2)} \qquad \overline{X}_i^{(0)}, \overline{X}_i^{(1)}, \overline{X}_i^{(2)} \text{ are all of Order(1)}$$

$$\overline{X}_j = \overline{X}_j^{(0)} + \varepsilon\overline{X}_j^{(1)} + \varepsilon^2\overline{X}_j^{(2)} \qquad \overline{X}_j^{(0)}, \overline{X}_j^{(1)}, \overline{X}_j^{(2)} \text{ are all of Order(1)}$$

Hence, substitute the above series into the original differential equation, will yield:

$$\left(\frac{\partial}{\partial\overline{\tau}_0} + \varepsilon\frac{\partial}{\partial\overline{\tau}_1} + \varepsilon^2\frac{\partial}{\partial\overline{\tau}_2}\right)(\overline{T}_k^{(0)} + \varepsilon\overline{T}_k^{(1)} + \varepsilon^2\overline{T}_k^{(2)}) = G_k^{(0)} + \varepsilon G_k^{(1)} + \varepsilon^2 G_k^{(2)}$$

$$\therefore \quad \frac{\partial\overline{T}_k^{(0)}}{\partial\overline{\tau}_0} + \varepsilon\left(\frac{\partial\overline{T}_k^{(0)}}{\partial\overline{\tau}_1} + \frac{\partial\overline{T}_k^{(1)}}{\partial\overline{\tau}_0}\right) + \varepsilon^2\left(\frac{\partial\overline{T}_k^{(0)}}{\partial\overline{\tau}_2} + \frac{\partial\overline{T}_k^{(1)}}{\partial\overline{\tau}_1} + \frac{\partial\overline{T}_k^{(2)}}{\partial\overline{\tau}_0}\right) + O(\varepsilon^3) = G_k^{(0)} + \varepsilon G_k^{(1)} + \varepsilon^2 G_k^{(2)}$$

$$\varepsilon\frac{\partial\overline{X}_i^{(0)}}{\partial\overline{\tau}_0} + \varepsilon^2\left(\frac{\partial\overline{X}_i^{(0)}}{\partial\overline{\tau}_1} + \frac{\partial\overline{X}_i^{(1)}}{\partial\overline{\tau}_0}\right) + O(\varepsilon^3) = F_i^{(0)} + \varepsilon F_i^{(1)} + \varepsilon^2 F_i^{(2)}$$

$$\varepsilon^2\frac{\partial\overline{X}_j^{(0)}}{\partial\overline{\tau}_0} + O(\varepsilon^3) = F_j^{(0)} + \varepsilon F_j^{(1)} + \varepsilon^2 F_j^{(2)}$$

Separating terms with respect to $O(1)$, $O(\varepsilon)$ and $O(\varepsilon^2)$, will get systems of equation below:

Order (1):

$$\frac{\partial\overline{T}_k^{(0)}}{\partial\overline{\tau}_0} = G_k^{(0)} \qquad F_i^{(0)} = 0 \qquad F_j^{(0)} = 0$$

Order (ε):

$$\frac{\partial\overline{T}_k^{(1)}}{\partial\overline{\tau}_0} = G_k^{(1)} - \frac{\partial\overline{T}_k^{(0)}}{\partial\overline{\tau}_1} \qquad \frac{\partial\overline{X}_i^{(0)}}{\partial\overline{\tau}_0} = F_i^{(1)} \qquad F_j^{(1)} = 0$$

Order (ε^2):

$$\frac{\partial\overline{T}_k^{(2)}}{\partial\overline{\tau}_0} = G_k^{(2)} - \frac{\partial\overline{T}_k^{(1)}}{\partial\overline{\tau}_1} - \frac{\partial\overline{T}_k^{(0)}}{\partial\overline{\tau}_2} \qquad \frac{\partial\overline{X}_i^{(1)}}{\partial\overline{\tau}_0} = F_i^{(2)} - \frac{\partial\overline{X}_i^{(0)}}{\partial\overline{\tau}_1} \qquad \frac{\partial\overline{X}_j^{(0)}}{\partial\overline{\tau}_0} = F_j^{(2)}$$

For each of the above *Order* system, the dependent variables of the lower-order systems do not appear in the RHS of the said system. It is integrated independently in time τ_0 to supply its value at $\tau_0 + \Delta\tau_0$ for the RHS of the lower-order systems. So, right of the bat, one appreciates the fact that the dependent variables are not solved simultaneously but in succession, greatly facilitating the computational effort.

RESULTS OF SIMULATION OF LHP DYNAMICS – HOPF BIFURCATION

The current research is in an initial phase of a far-reaching investigation of the LHP dynamical behaviors for long-duration operations. A FORTRAN computer code was developed – utilizing

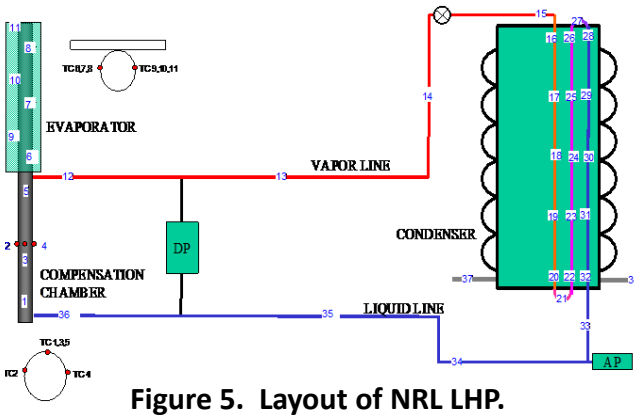

Figure 5. Layout of NRL LHP.

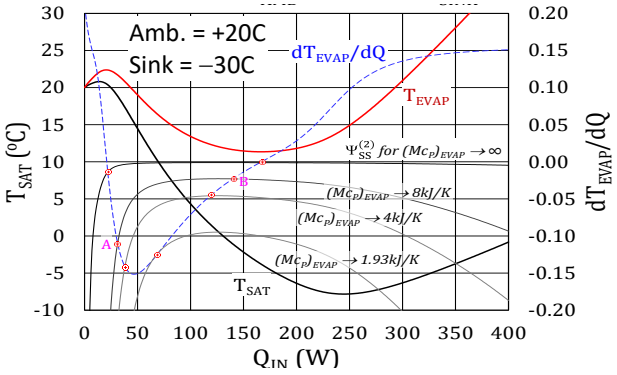

Figure 6. NRL LHP Equilibrium States.

the numerical scheme outlined in the previous section – specifically for this study. Therefore, the first step was to assess the code predictions against the available test data from various LHP systems of different designs, sizes, and working fluid. Excellent model verification was obtained for all correlated data (see Ref. 11 & 12). Due to limited space of this paper, the only LHP chosen for the data presentation of the current study came from the same unit that underwent testing extensively at NRL and NASA Goddard since 1997[17]. The latest tests, performed in 2017 having an 8kg mass attached to the LHP evaporator, provided the bulk of data for the present research. Figure 5 shows the layout of the NRL LHP and Table 1 lists the main components' physical dimensions and properties. The LHP natural curves T_{SAT} & T_{EVAP} vs. T_{SINK} = -30°C and T_{AMB} = +20°C are given in Figure 6. Hence, the LHP linear stability theory states that the NRL LHP unstable operation – with 8kJ/K of attached thermal mass to the evaporator – occurs in the power regime between 31-143W causing the temperatures to oscillate. Outside this range, the temperatures shall be able to reach steady state. In other words, Point A and Point B are the *Hopf* bifurcation points[18]. So, the plan is to start the numerical investigation with a low power operation just on

Table 1. Physical Dimension and Wick Properties of NRL LHP Components

Evaporator			
Primary Wick		*Casing/Saddle, 1st Wick, and Attached Thermal Mass*	
Material:	Sintered Powder Nickel	Thermal Mass of Heater Plate + Saddle + Casing:	1,575J/K
Outer Diameter:	24.21mm (0.950")	Thermal Mass-to-Vapor Conductance G_E:	*35.80 W/K*
Inner Diameter:	*9.525mm (0.375")*	*Vapor Grooves*	
Active Length:	0.3048m (12")	Number of Channels:	*4*
Max. Pore Radius:	1.3µm	Hydraulic Diameter:	*0.05"*
Permeability:	$1.3 \times 10^{-14} m^2$		
Effective Conductivity:	*7.80W/m-K*		
Transport Lines			
Vapor Line		*Liquid Line*	
Outer Diameter:	4.76mm	Outer Diameter:	4.76mm
Wall Thickness:	0.508mm	Wall Thickness:	0.508mm
Length:	1.524m	Length:	1.96m (incl. bayonet)
Condenser		Reservoir	
Number of Parallel Passes	1	Outer Diameter:	25.4mm
Heat Exchanger Tubing		Wall Thickness:	*1.27mm*
Inner Diameter:	3.744mm	Active Length:	0.127m
Length:	2.032m (80")	Thermal Mass $(Mc_P)_R$:	*135.80J/K*
Conductance $G_C^{(MAX)}$:	*12.00W/K*	Conductance G_R:	*16.50W/K*

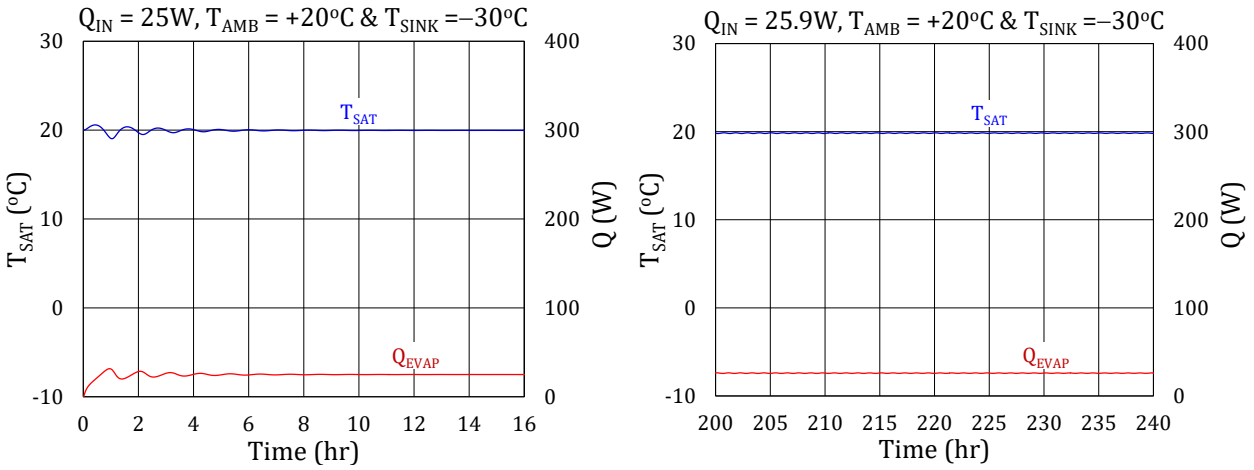

Figure 7. Model Simulation of NRL LHP 25W and 25.9W Operations.

the left of Point A, say, 25W. The task will continue with the power input gradually increased until the oscillations completely disappear. If the results turn out positive, the validity of the linear stability theory is further re-affirmed. Let us first define what a phase state is and explain how a state of a dynamical system evolves in it. A "state" uniquely defines the system operational characteristics at a given time, represented by heat transport Q_{EVAP}, sink temperature T_{SINK}, ambient temperature T_{AMB}, saturation temperature T_{SAT}, evaporator temperature T_{EVAP}, and time. So, the LHP phase space is a 6-dimension domain. So, when T_{SAT} and T_{EVAP} are plotted against Q_{EVAP} on the same graph, the pair of (T_{SAT}/T_{EVAP}) associated with a value of Q_{EVAP} defines one LHP state in constant (T_{SINK}/T_{AMB}) environment. It would be easier to see how a LHP state evolves with time, should a third axis for time be added to the (T_{SAT}/T_{EVAP}) vs. Q_{IN} curve. Better still, for constant (T_{SINK}/T_{AMB}), the time evolution of the LHP is displayed, hereafter, in two separate plots – T_{SAT} vs. Q_{EVAP} and T_{SAT} & Q_{EVAP} vs. time – placed side-by-side.

Figure 7 displays the results from the first run made with the LHP initially dormant: Q_{EVAP} = 0, T_{SAT} = +20°C, T_{AMB} = +20°C, and T_{SINK} = -30°C. Power of 25W was applied to the evaporator to start the LHP. The loop started and T_{SAT} oscillated with an amplitude of less than 1K but began to

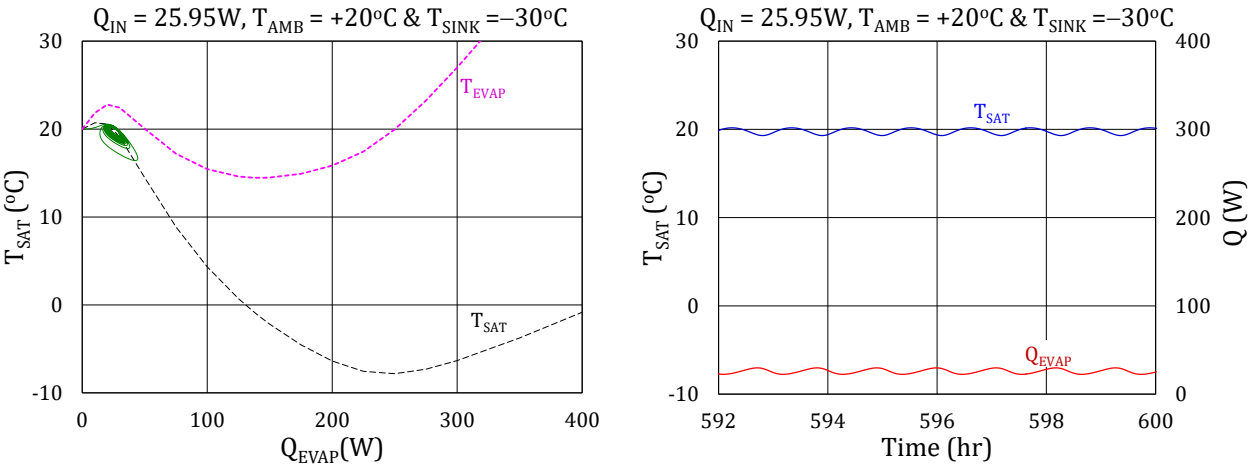

Figure 8. Model Simulation of NRL LHP with 25.95W Operations – First Hopf Point.

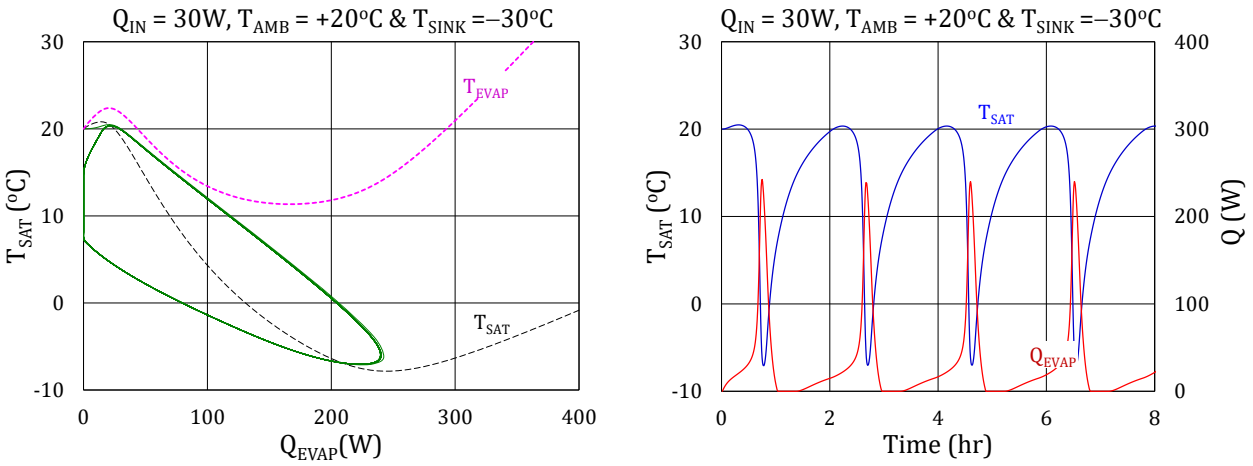

Figure 9. Model Simulation of NRL LHP with 30W Operations – Instability.

decay and eventually vanished after 5 cycles. A cycle in this operation (oscillation period) lasted 1.1 hours. Nevertheless, the LHP was able to reach steady state with T_{SAT} = +19.97°C. The power input was increased to 25.9W and the model was re-run. The results are displayed also in Figure 7. The initial amplitude/period became larger but it took more than 240 hours to damp out. The study inched up only by 0.05W to 25.95W but the search for the first Hopf bifurcation point was

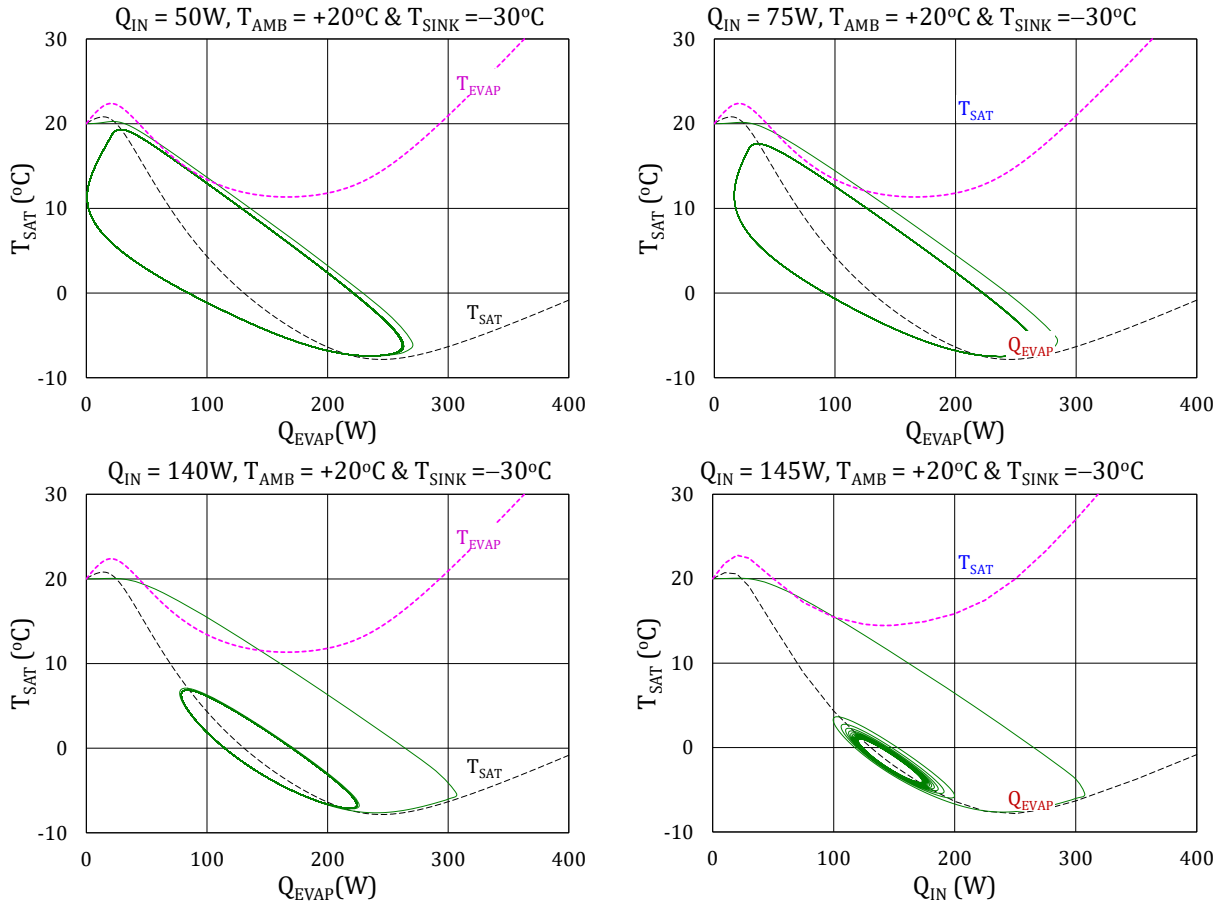

Figure 10. Model Simulation of NRL LHP with 50W, 75W, 140W, 145W Operations – Instability.

a success. Even with a tiny change of 0.05W, the LHP went from a stable operation to a persistent oscillatory (0.45K/1.1hr) state of time evolution as Figure 8 revealed. With another 4.05W increase, the same run was made with 30W. Figure 9 disclosed sudden jumps in both amplitude and period to 27K/2hrs. Since the first transition point was found, the task soldiered on with a large step-up of power every time. Figures 10 presents the LFHA results in the 50W, 75W, 140W and 145W operations. Since the oscillations did not go away at 145W, two more power levels, 147W and 150W, were simulated and the plots in phase space are given in Figure 11. The second stability/instability transition point (second Hopf) did indeed occur between 145W and 147W.

SUMMARY AND DISCUSSION

Unexpected oscillatory behaviors of LHP operations in certain regimes prompted an investigation of the technology suitability for space applications beyond the known working envelope. LHP testing or other experimental studies are time-consuming and expensive to cover all expected orbital conditions, the responsible TCS engineers must rely on well-established theories to model/simulate the proposed LHP system before committing it to the design for flight. Due to the complexity and convoluted nature of the LHP system thermal/fluid interaction, analytical modeling is not everyone's cup of tea! Recognizing the importance of LHPs to the space business,

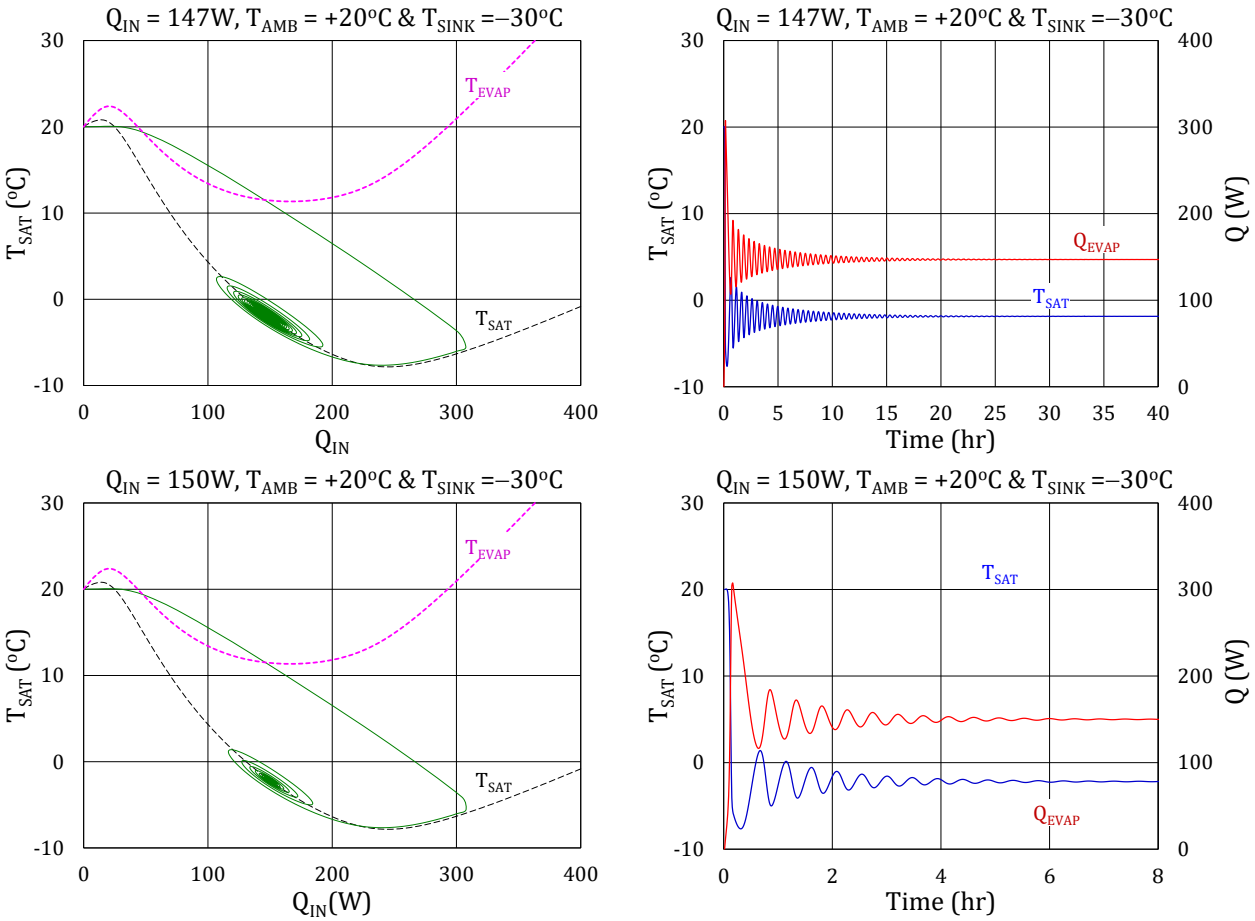

Figure 11. Model Simulation of NRL LHP with 147W, 150W Operations – 2nd Hopf Point.

research projects – dedicated to the understanding dynamical system characteristics of LHPs in different performance regimes – began to appear. The first LHP linear stability/instability theory was able to establish criteria for stable/unstable operation, which had proven to be a great success. Nevertheless, being a linearized approximation, the theory could only say whether a particular set of operating conditions would lead to unstable performance but not capable of predicting the system behaviors when it did encounter instability. Furthermore, in many cases, temperature oscillations with acceptable amplitudes/frequency to usage at hand are still considered for flight. The necessity for efficient numerical methods to simulate accurately the long-duration LHP operations becomes apparent. Recognized for some time that the LHP thermal/fluid dynamics involved multiple distinct time scales, the Method of Multiple Scales of the perturbation theory was indeed suggested as a suitable numerical scheme. Accordingly, the author successfully developed a fairly simple computer code for the simulations that correlated with the available test data very well. As it turned out, the LHP operations share every bit of the same operational features of other dynamical systems in many diverse disciplines from biology, chemistry, ecology, economics, physics to sociology, stock market, and even foreign policy. They all possess to some mechanism of *predator-prey* struggle[19]. An example[20] is given in Figure 12.

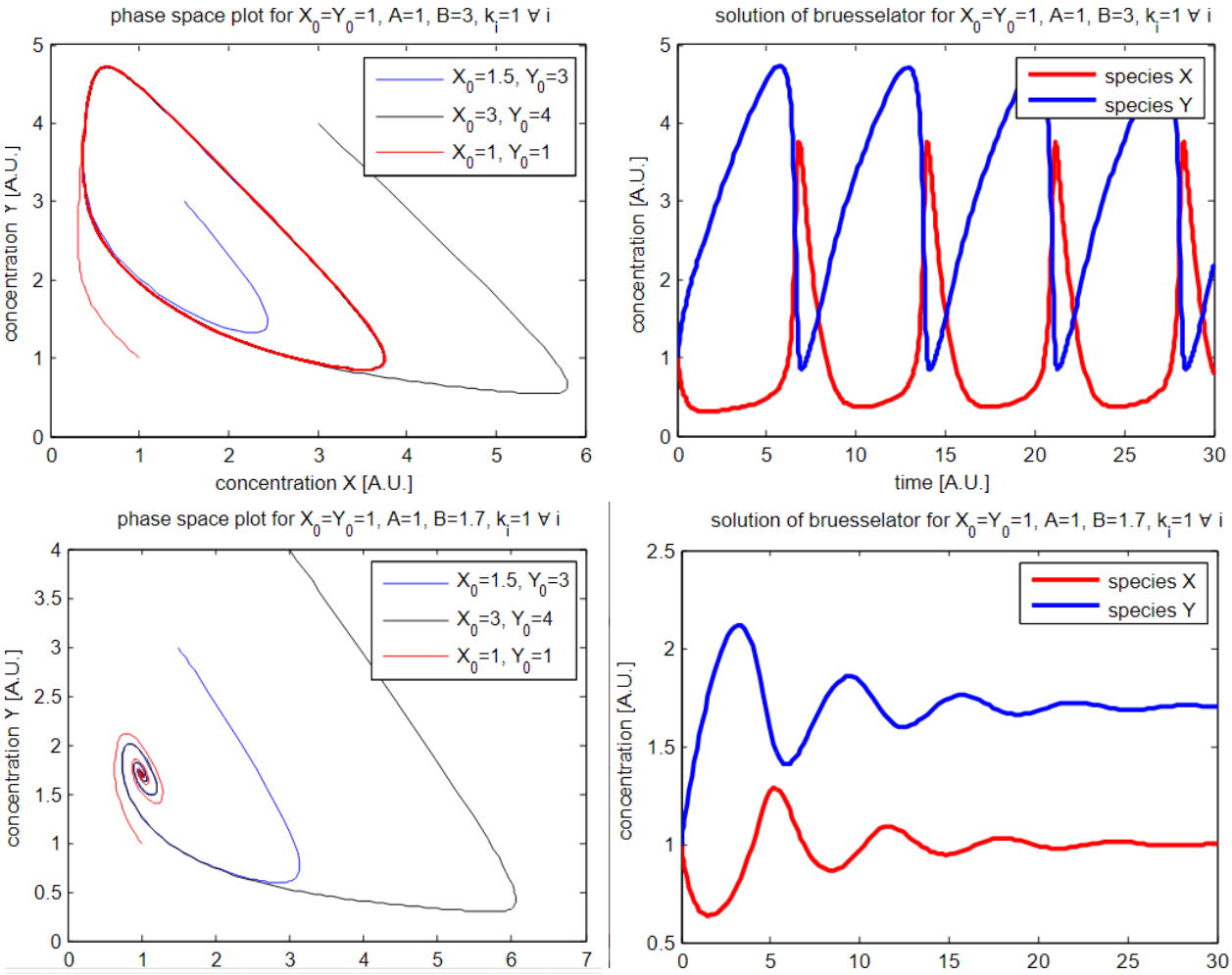

Figure 12. Similar Characteristics in Brusselator Model for Autocatalytic Reaction.

CONCLUSION

Results of the research presented in this paper proved beyond a reasonable doubt that the LHP innerworkings are far more complex and difficult to comprehend than its simplistic appearance. Despite years of experience and successful space programs to boost, it would be too irresponsible for anyone who declared it a "fully flight qualified" technology (even with the room temperature LHPs). As challenging as it is to vet the technology in untested operational regimes for behaviors/ characteristics that are potentially detrimental to the LHP in-service operations. Fortunately, the present study attests that the underlined LHP thermal/fluid interaction fundamentally forms a dynamical system, which exhibits basically the same phenomena as those in many other diverse disciplines. At the very least, the ample knowledge obtained in the field of *Dynamical Systems* offers a roadmap for future analytical/experimental investigations of the LHP system.

CONTACT

Dr. Triem T. Hoang
President
TTH Research Inc.
Clifton, VA 20124
703-344-4575
thoang7291@aol.com

REFERENCES

1. Ku, J., "Operational Characteristics of Loop Heat Pipes," Paper No. 1999-01-2007, Proceedings of the 29th International Conference on Environmental Systems, Denver, CO, 1999.
2. Hoang, T. and J. Ku, "Heat and Mass Transfer in Loop Heat Pipes," Paper No. HT2003-47366, Proceedings of the 2003 ASME Summer Heat Transfer Conference, Las Vegas, NV, 2003.
3. Baker, C., E. Grob, T. McCarthy, M. Nikitkin, and W. Ancarrow, "Geoscience Laser Altimetry System (GLAS) On-Orbit Flight Report on the Propylene Loop Heat Pipes (LHPs)," Space Technology and Applications International Forum STAIF 2004, Albuquerque, NM, 2004.
4. Choi, M. "SWIFT BAT Loop Heat Pipe Thermal System Characteristics and Ground/Flight Operation Procedure," Paper No. AIAA 2003-6077, 1st International Energy Conversion Engineering Conference, 17 - 21 August 2003, Portsmouth, Virginia.
5. Rodriguez, J. and A. Na-Nakornpanom, "Investigation of Transient Temperature Oscillations of a Propylene Loop Heat Pipe," Paper No. 01ICES-74, International Conference on Environmental Sciences (ICES), 2001.
6. Ku, J., "High Frequency Low Amplitude Temperature Oscillations in Loop Heat Pipe Operation," Paper No. 2003-01-2387, SAE 33rd International Conference on Environmental Sciences (ICES), Vancouver, British Columbia, Canada, July 7-10, 2003.

7. Hoang, T. and R. Baldauff, “Stability Theory for Loop Heat Pipe Design, Analysis and Operation,” Paper No. ICES-2015-14, Proceedings of the 45th International Conference on Environmental Systems, Bellevue, WA, July 12-16, 2015.
8. Hoang, T. and J. Ku, “Theory of Hydrodynamic Stability for Capillary Pumped Loops,” Proceedings of ASME 1995 National Heat Transfer Conference, ASME HTD Vol 307, pp. 33-40, Portland, OR, Aug. 6-9, 1995.
9. Ku, J. and T. Hoang, “An Experimental Study of Pressure Oscillation and Hydrodynamic Stability in a Capillary Pumped Loop,” Proceedings of ASME 1995 National Heat Transfer Conference, ASME HTD Vol 307, pp. 25-32, Portland, OR, Aug. 6-9, 1995.
10. Hoang, T., “Linear Stability Analysis for Loop Heat Pipe Operations,” Paper No. 2019ICES201-89, Proceedings of the 49th International Conference on Environmental Systems, Boston, MA, July 7-11, 2019.
11. Hoang, T., R. Baldauff, and C. Tiu, “Verification of Loop Heat Pipe Stability Theory – Part I Low-Frequency/High-Amplitude Oscillations,” Paper No. ICES-2015-39, 45th International Conference on Environmental Sciences (ICES), Bellevue, Washington, USA, July 12-16, 2015.
12. Hoang, T. and R. Baldauff, “Verification of LHP Stability Theory – Part II High-Frequency/Low-Amplitude Temperature Oscillations,” 26th Thermal and Fluids Analysis Workshop, Silver Spring, MD, August 3-7, 2015.
13. Nayfeh, A.H., Introduction to Perturbation Techniques, John Wiley and Sons, 1993 Edition.
14. Hoang, T. and R. Baldauff, “Stability and Oscillations in Loop Heat Pipe Operation: A Classic Nonlinear Dynamics Problem,” Proceedings of the 2011 International Two-Phase Thermal Control Workshop, College Park, MD, Oct. 31 – Nov. 2, 2011.
15. Hoang, T., R. Baldauff, and K. Cheung, “Start-Up Behavior of an Ammonia Loop Heat Pipe,” Paper No. AIAA 2005-5630, 3rd International Energy Conversion Engineering Conference, 15 - 18 August 2005, San Francisco, CA.
16. Naidu, D., “Singular Perturbations and Time Scales in Control Theory and Applications: An Overview,” Dynamics of Continuous, Discrete and Impulsive Systems, Series B: Applications & Algorithms, pp. 233-278, Watcom Press, 2002.
17. Cheung, K., T. Hoang, J. Ku, and T. Kaya, “Thermal Performance and Operational Characteristics of Loop Heat Pipe (NRL LHP),” SAE Paper No. 981813, 28th International Conference on Environmental Systems, Danvers, Massachusetts, 1998.
18. Guckenheimer, J., M. Myers, and B. Sturmfels, "Computing Hopf Bifurcations I," SIAM Journal on Numerical Analysis, Volume 34, No. 1, pp. 1-21 (1997).
19. Brauer, F. and C. Castillo-Chavez, Mathematical Models in Population Biology and Epidemiology, Springer-Verlag, Heidelberg, 2000.
20. McDowell, M.P., “Mathematical Modeling of the Brusselator,” Dept. of Aerospace and Mechanical Engineering, University of Notre Dame, Notre Dame, IN, 2008.